Check for updates

© IWA Publishing 2018
753

Water Practice & Technology Vol 13 No 4
doi: 10.2166/wpt.2018.088

Removal of arsenate by electrocoagulation reactor using aluminum ball anode electrodes

A. Y. Gören[a,*], M. S. Öncel[b], E. Demirbas[c], E. Şık[d] and M. Kobya[b]

[a] Department of Environmental Engineering, İzmir Institute of Technology, 35430, İzmir, Turkey

[b] Department of Environmental Engineering, Gebze Technical University, 41400, Gebze-Kocaeli, Turkey

[c] Department of Chemistry, Gebze Technical University, 41400, Gebze-Kocaeli, Turkey

[d] Tübitak Marmara Research Center, Environment and Cleaner Production Institute, 41470 Gebze-Kocaeli, Turkey

*Corresponding author. E-mail: yagmurgoren@iyte.edu.tr

Abstract

The aim of this research was to remove arsenate (As(V)) from groundwater using an air-injected electrocoagulation (EC) reactor with aluminum (Al) ball anodes. The effects of seven operating variables – initial pH, applied current (i), operating time (t_{EC}), initial As(V) concentration (C_o), Al ball anode diameter (d_p), reactor column height (h), and airflow rate (Q_{air}) were investigated with a Box-Behnken statistical experimental design. ANOVA results from the quadratic model equations indicated that the model fitted very well with the experimental data for the responses, which were removal efficiency, operating cost (OC), As(V) adsorption capacity, and effluent concentration ($R^2 \geq 0.87$). The most effective parameters were applied current, operating time, and anode height for As(V) removal efficiency in the EC reactor, while initial pH, Al anode diameter, and air flow rate had limited effect on removal. The model predicted a residual As(V) concentration below 10 μg/L under the optimum operating conditions (pH 7.03, 0.29 A, 10.5 min, d_p 7.5 mm, 613.4 μg/L, h 5.1 cm, and Q_{air} 6.4 L/min). The maximum As(V) removal efficiency and minimum OC in the EC process were almost 99% and 0.442 $/m^3, respectively.

Key words: Al ball anodes, arsenate removal, Box-Behnken design, electrocoagulation

INTRODUCTION

Arsenic contamination is a global problem because many people suffer from excessive arsenic content in drinking water sources (Murcott 2009; Nordstrom 2015). People in countries such as Argentina, Bangladesh, Cambodia, Chile, China, Finland, Hungary, India, Japan, Mexico, Nepal, Turkey, United States, and Vietnam can be exposed to arsenic concentrations exceeding the 10 μg/L maximum recommended by WHO (2011) (Ng *et al.* 2003; Murcott 2009; Ravenscroft *et al.* 2009). It is estimated that between 35 and 77 million of Bangladesh's 125 million inhabitants are at risk from drinking water contaminated with natural inorganic arsenic (Smith *et al.* 2000).

It is known that there is arsenic pollution in drinking water in some parts of western Turkey particularly; natural waters contain much higher levels of arsenic than the maximum level recommended by WHO. Balikesir-Bigadiç, Kütahya-Emet, and Hisarcik in Turkey are affected by natural arsenic dissolved from minerals like realgar and orpiment in a borate-bearing clay zone and colemanite boron mineral nodules (Colak *et al.* 2003).

Arsenic contamination of water arises from the dissolution and/or oxidation of minerals like realgar, orpiment, and arsenopyrite, from desorption in oxidizing environments, and reductive desorption and dissolution (Smedley & Kinniburgh 2002; Ravenscroft *et al.* 2009). Drinking water containing arsenic in the long term may cause skin cancer and lesions such as lung, bladder, and kidney cancers,

Downloaded from http://iwaponline.com/wpt/article-pdf/13/4/753/527586/wpt0130753.pdf
by guest

Water Practice & Technology Vol 13 No 4
doi: 10.2166/wpt.2018.088

hyperkeratosis, hyperpigmentation (melanosis), hypopigmentation, black foot and Bowen's diseases, neurological effects, hypertension and cardiovascular disease, and diabetes mellitus (Çöl *et al.* 1999; Smith *et al.* 2000; Tseng *et al.* 2007). WHO and the US Environmental Protection Agency (USEPA) reduced the maximum recommended arsenic concentration in drinking water from 50 to 10 μg/L (USEPA 2001; WHO 2011).

Electrocoagulation (EC) has been the focus of increasing interest recently for arsenic removal, compared to conventional methods, owing to its high removal efficiency, reduced sludge volumes, process compactness, cost-effective removal to trace levels, and lack of need for chemical reagents for pre-oxidation of arsenite (As(III) to As(V)) (Chen *et al.* 2000; Kobya *et al.* 2006; Ulu-Kac *et al.* 2017). The literature shows that rod and plate Al and/or Fe electrodes are generally used for arsenic removal in EC reactors (Kumar *et al.* 2004; Gomes *et al.* 2007; Amrose *et al.* 2009; Gunduz *et al.* 2010; Lakshmanan *et al.* 2010; Ucar *et al.* 2013). However, rod and plate type anodes offer some disadvantages because of potential difficulties in operation and low surface areas. For this reason, an air-fed EC reactor using Fe-ball anodes was designed and optimized recently, to study the operating parameters and eliminate problems (Sık *et al.* 2015). They showed that ball-shaped iron anodes in the reactor performed as effectively as the plate- and rod-shaped anodes (Kobya *et al.* 2015; Sık *et al.* 2017a, 2017b).

In this study, a fixed-bed EC reactor using aluminum ball anodes with air injection was evaluated for arsenic (As(V)) removal from groundwater. The effects of parameters such as operating time, applied current, initial pH, initial arsenate concentration, air flow rate, ball anode size, and anode height in the EC reactor were investigated using the three-level Box-Behnken Design (BBD) experimental method.

ARSENIC REMOVAL BY EC USING AL ANODES

Electrocoagulation involves both dissolution of metal from the sacrificial anodes and hydroxyl ion and hydrogen gas formation at the cathode (Chen *et al.* 2000; Holt *et al.* 2002; Garcia-Lara & Montero-Ocampo 2010). Hydrogen gas evolution enhances solution mixing and hence coagulant flocculation in EC reactors. Aluminum and iron, the sacrificial electrode materials, are most commonly preferred in EC, because they are inexpensive and readily available, and allow the formation of mainly amorphous hydroxides, metal oxides, and oxyhydroxides that have remarkable features for the adsorption and co-precipitation of soluble species (Holt *et al.* 2002). Aluminum, for instance, when released electrochemically, reacts with the hydroxyl ions from the cathode to form aluminum hydroxide ($Al(OH)_3$; i.e. bayerite and gibbsite). The main anode and cathode reactions (Chen *et al.* 2000; Kobya *et al.* 2011) are:

$$\text{Anode: } Al_{(s)} \rightarrow Al^{3+} + 3e^- \quad (1)$$

$$\text{Cathode: } 3H_2O + 3e^- \rightarrow 3/2H_{2(g)} + 3OH^- \quad (2)$$

During EC the electrochemically dissolved aluminum anode produces Al^{3+} ions. According to Faraday's law, the charge loading (the product of the current applied and the EC duration) determines both the Al^{3+} (coagulant) dosage and the $H_{2(g)}$ gas bubble production rates (Chen *et al.* 2000). As the Al^{3+} concentration increases, monomeric species like $Al_2(OH)_2^{4+}$, $Al(OH)^{2+}$, $Al(OH)_2^+$, and $Al(OH)_4^-$, and polymeric species such as $Al_{13}O_4(OH)_{24}^{7+}$, $Al_{13}(OH)_{34}^{5+}$, $Al_7(OH)_{17}^{4+}$, $Al_8(OH)_{20}^{4+}$, and $Al_6(OH)_{15}^{3+}$ are formed, and aluminum hydroxide precipitates (Holt *et al.* 2002; Kobya *et al.* 2011):

$$xAl^{3+} + yH_2O \rightarrow Al_x(OH)_y^{3x-y} + yH^+ \quad (3)$$

$$\text{Monomeric and polymeric } Al_x(OH)_y^{3x-y} \text{species} \rightarrow Al(OH)_3 \quad (4)$$

Downloaded from http://iwaponline.com/wpt/article-pdf/13/4/753/527586/wpt0130753.pdf
by guest

Water Practice & Technology Vol 13 No 4
doi: 10.2166/wpt.2018.088

As the Al hydroxide species precipitate, their amorphous nature increases the surface area available for arsenate species adsorption and thus arsenic removal efficiency. On the other hand, the negatively charged As(V) species that dominate in relation to pH are AsO_4^{3-} at pH > 12.4;$H_2AsO_4^-$ at 3.6 < pH 7.2, and $HAsO_4^{2-}$ at 7.2 < pH < 12.4. (Vaclavikova *et al.* 2008).

$Al(OH)_{3(s)}$ is an amphoteric compound whose point of zero charge (pzc) is about pH 7.7 to 9.4 (Blangenois *et al.* 2004). It can be negatively or positively charged in solution, depending on whether pH < pzc or > pzc. $H_2AsO_4^-$ and $HAsO_4^{2-}$ are the predominant species at pH 6 to 9, and $Al(OH)_{3(s)}$ is positive, which enhances As(V) adsorption. Therefore, $Al(OH)_{3(s)}$ and $Al_2O_{3(s)}$ flocs are believed to adsorb $H_2AsO_4^-$ and $HAsO_4^{2-}$ ions at pH 6 to 9 in EC (Vasudevan *et al.* 2010; Kobya *et al.* 2011; Alcacio *et al.* 2014). At pH below ~9 in EC, $Al(OH)_4^-$, which is soluble, is dominant and useless for arsenate removal.

$$Al^{3+} + 4OH^- \rightarrow Al(OH)_4^- \tag{5}$$

The soluble arsenic species arising from co-precipitation reactions during EC are incorporated into a growing aluminum hydroxide phase by adsorption, occlusion, or inclusion. Monomeric and polymeric Al^{3+} species (i.e., $Al_2O_{3(s)}$ and $Al(OH)_{3(s)}$) also form arsenate complexes. Finally, soluble arsenic adheres electrostatically to the external surfaces of insoluble aluminum hydroxide precipitates (Bilici-Baskan & Pala 2010; Vasudevan *et al.* 2010).

Adsorption reactions:

$$Al(OH)_{3(s)} + H_2AsO_4^- \text{or } HAsO_4^{2-} \rightarrow [Al(OH)_3{*}H_2AsO_4^- \text{or } HAsO_4^{2-}]_{(s)} \tag{6}$$

$$Al_2O_3 + H_2AsO_4^- \text{or } HAsO_4^{2-} \rightarrow [Al_2O_3{*}H_2AsO_4^- \text{or } HAsO_4^{2-}]_{(s)} \tag{7}$$

Co-precipitation reactions:

$$xAl^{3+} + (3x-y)OH^- + yHAsO_4^{2-} \rightarrow Al_x(OH)_{(3x-y)} - (HAsO_4)_{y(s)} \tag{8}$$

$$Al(OH)_3 + H_2AsO_4^- + H^+ \rightarrow [Al(OH)_2 - H_2AsO_4]_{(s)} + H_2O \tag{9}$$

$$Al(OH)_3 + HAsO_4^{2-} + 2H^+ \rightarrow [Al(OH) - HAsO_4]_{(s)} + 2H_2O \tag{10}$$

$$\equiv Al - OH_{(s)} + H_2AsO_4^- \text{or } HAsO_4^{2-} \rightarrow \equiv Al - OAs(O)_2(OH)_{(s)}^- + OH^- \tag{11}$$

where the symbol ≡ describes the bonds of cations with the surfaces of solids.

MATERIALS AND METHODS

Groundwater characterization

Groundwater was collected from deep wells in Kocaeli, Turkey, and kept in a 5 m^3, high density polyethylene (HDPE) container throughout the experiments. The groundwater chemistry was determined using American Public Health Association (APHA) standard methods (APHA 2005). The groundwater characterization results revealed – pH 7.6, electrical conductivity 1,055 μS/cm, total hardness 418 mg-$CaCO_3$/L, TOC 5 mg/L, turbidity 1 NTU, and 0.006 mg-Mn/L, 22 mg-Na/L, 152 mg-Ca/L, 15 mg-Mg/L, 127 mg-Cl/L, 94.2 mg-SO_4/L, 24 mg-NO_3/L and 10.2 mg-SiO_4/L. Fe, Al, P, F and As were not detected. The arsenic solution was prepared daily by dissolving sodium arsenate ($Na_2HAsO_4.7H_2O$) at various concentrations (100, 550, and 1,000 μg/L).

Downloaded from http://iwaponline.com/wpt/article-pdf/13/4/753/527586/wpt0130753.pdf
by guest

Water Practice & Technology Vol 13 No 4
doi: 10.2166/wpt.2018.088

Specifications – air-injection fixed-bed EC reactor

Figure 1 includes a schematic diagram of the EC reactor. This consists of a round base unit and cylindrical Plexiglas tube, containing both a cylindrical titanium cathode and another Plexiglas tube holding the Al-ball anodes. The base (45 mm thick) is of 150 mm diameter and has equidistant 2 mm holes drilled in it. The cylindrical Plexiglas tube/cell (254 × 100 × 5 mm) and an air feed diffuser stand on the base. The cylindrical titanium cathode (250 × 70 × 1 mm), with 5 mm diameter holes, and second Plexiglas cylinder (250 × 60 × 5 mm), with equidistant, 2 mm holes, stand inside the base unit. The 2 to 8 mm diameter Al-ball anodes and a stainless steel rod are placed in the center of the 60 mm diameter Plexiglas column. The titanium cathode and Al-ball anodes, which are in contact with the stainless steel rod, are connected to a DC power supply (Agilent 6675A, 0-120 V/0-18A). This EC configuration provides a significant increase in the surface area of the anode materials.

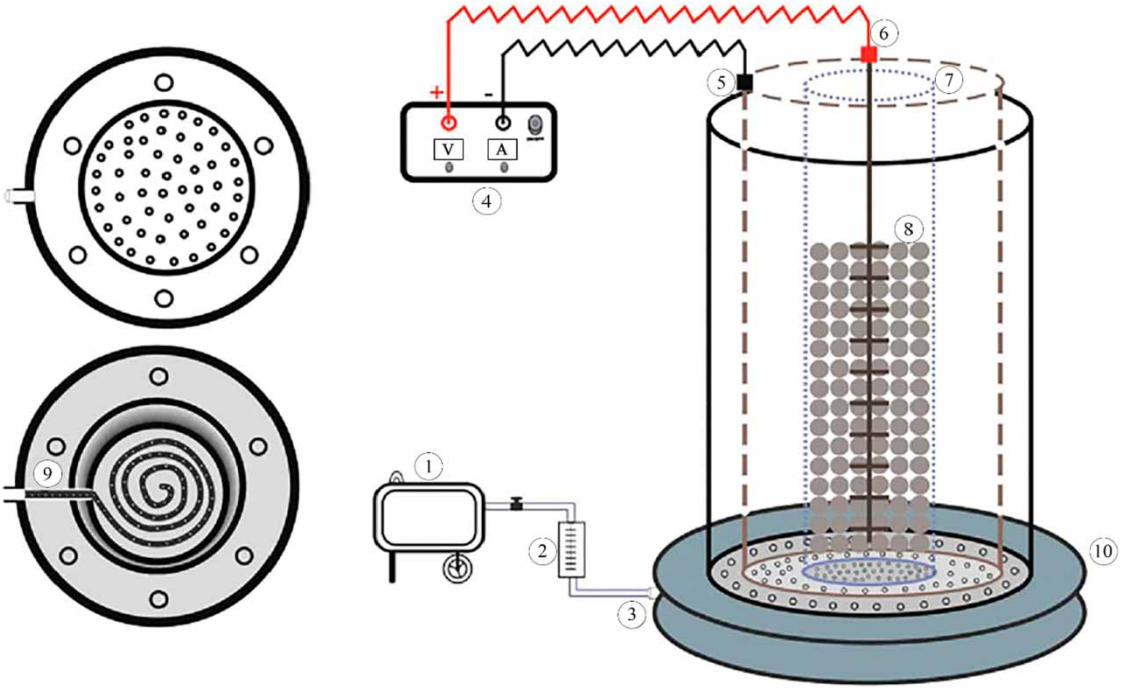

Figure 1 | Schematic diagram of the fixed-bed EC reactor: (a) air diffuser unit; and (b) 1. Air compressor, 2. Air flow meter, 3. Air diffuser line, 4. DC power supply, 5. Cylindrical Ti cathode, 6. Supporting rod for anode material, 7. Inner Plexiglas cylinder, 8. Al-ball anodes, 9. Air diffuser unit, 10. EC reactor.

Experimental procedure

The operating variables in the experiments were determined according to BBD statistical experiment design. The reactor was fed with 0.8 L of groundwater at the start of each run. It was operated for different periods and all experiments were conducted in batch mode. During the experiments, voltage input from the DC power supply was recorded to determine energy consumption. Samples were collected at specified intervals and filtered through 0.45 μm Millipore membranes prior to analysis. The weight of the Al-ball anodes was measured before and after the experiment. The experiments were repeated three times and averaged data used.

Experimental design

BBD involves, essentially, three main steps – checking the adequacy of the model and predicting the response, estimating the coefficients in a mathematical model, and performing the minimum number

Downloaded from http://iwaponline.com/wpt/article-pdf/13/4/753/527586/wpt0130753.pdf
by guest

Water Practice & Technology Vol 13 No 4
doi: 10.2166/wpt.2018.088

of well-chosen, statistically designed experimental runs. The statistical design and data analysis program 'Design Expert trial version 8.0.4.1' (Stat-Ease, Inc., Minneapolis, MN, USA) was used. In this study, seven factors with three levels of BBD surface experimental response were chosen to optimize process variable influence. The independent operating variables were – initial pH (pH_i: x_1), applied current (i: x_2), EC time (t_{EC}: x_3), Al-anode ball size at the start of the experiment (d_p: x_4), As(V) concentration (C_0: x_5), anode height in the reactor (h: x_6) and air flow rate (Q_{air}: x_7). The variables' ranges and levels in the study are shown in Table 1.

Table 1 | Independent variables and levels

	Ranges and levels		
Independent variables	**Low (−1)**	**Middle (0)**	**High (+1)**
x_1: initial pH (pH_i)	5.5	7.0	8.5
x_2: applied current (i, A)	0.1	0.30	0.50
x_3: EC time (t_{EC}, min)	2	10	18
x_4: size of Al anode ball (d_p, mm)	5.0	7.5	10.0
x_5: As(V) concentration (C_0, μg/L)	100	550	1,000
x_6: anode height in reactor (h, cm)	2	5	8
x_7: air flow rate (Q_{air}, L/min)	2	6	10

The design program produced 62 experiments. As shown in Table 1, the independent variables were studied at three levels: coded (−1), (0), and (+1) for low, middle, and high, respectively. Six dependent parameters were analyzed and experimental results for arsenate removal efficiency (R_e, %), effluent arsenate concentration (C_f, μg-As/L), energy consumption (ENC, kWh/m^3), electrode consumption (ELC, kg/m^3), arsenate adsorption capacity (q_e, μg-As/mg-Al), and operating cost (OC, \$/m^3) were recorded. ENC was calculated using Equation (12):

$$ENC(\text{kWh/m}^3) = \frac{U \times i \times t_{EC}}{v} \tag{12}$$

where U is the cell potential, i the applied current, v the reactor volume, and t_{EC} the treatment period. When 96,500 Coulomb of electricity passes through reactor, one gram-equivalent of material is released or disappears from the electrodes. In this case, the concentration of Al in solution is calculated using Equation (13):

$$ELC(\text{kg/m}^3) = \frac{i \times t_{EC} \times M_w}{z \times F \times v} \tag{13}$$

where M_w is the atomic weight of Al ($M_{w,Al} = 26.98$ g/mol) and z the number of electrons transferred in the reaction ($z_{Al} = 3$). In the EC process, the main operating costs arise from the electricity and electrode materials (Daneshvar *et al.* 2006). Therefore, the operating cost (OC) was calculated on the basis of energy and electrode consumption:

$$OC(\$/\text{m}^3) = \alpha \times ENC + \beta \times ELC \tag{14}$$

where α is the unit energy price (0.19 \$/kWh) and β (15 \$/kg) the unit electrode price, both based on price indexes dated March 2018.

Downloaded from http://iwaponline.com/wpt/article-pdf/13/4/753/527586/wpt0130753.pdf
by guest

Water Practice & Technology Vol 13 No 4
doi: 10.2166/wpt.2018.088

RESULTS AND DISCUSSION

Response surface methodology

Response surface methodology (RSM) is a statistical technique used to optimize multi-variable experiments. One of the most common RSMs is BBD, which is a collection of mathematical and statistical techniques. BBD is used to determine the optimum conditions for a limited number of experiments.

Analysis of variance (ANOVA) was applied to evaluate the adequacy of the mathematical model statistically. The accuracy of the quadratic regression model was tested by using the values of R^2 and *F-value*. The ANOVA results – Table 2 – were used to verify the significant effects of process variables on the effluent As(V) concentration (C_f), As(V) removal efficiency, electrode consumption, energy consumption, and OC for Al-ball anodes. The coefficient of variance (CV) is the ratio of the standard error of estimate to the mean value of the observed response (as a percentage), and is considered reproducible when it is below 10%. Adequate precision (AP) compares the range of the predicted values at the design points to the average prediction error, and a value above 4.0 is desirable. The predicted residual error sum of squares (PRESS) is used in regression analysis to provide a summary measure of the fit of a model to sample observations. The *F-value*, the noise to response ratio, implies that the model is significant. F-values were 5.06 for R_e and 21.36 for *OC* for Al-ball anodes, respectively. *Prob* > *F* values below 0.0001 indicate that the model terms are statistically significant. In addition, the suitability of the model was evaluated using the coefficient and adjusted coefficient of determination, R^2, and *Adj-*R^2, respectively (Swamy *et al.* 2014). They were between 0.872 and 0.996, and 0.710 and 0.978, respectively – R^2 values were 0.91 for the effluent As(V) concentration and 0.96 for OC. These values, which were close to 1, justified the accuracy of the model by suggesting that it was highly significant. The *Adj-*R^2 values also indicate that the final prediction agreed well with the experimental results.

Table 2 | ANOVA results for the quadratic model

Responses	R^2	Adj-R^2	SD	CV	PRESS	F-value	Prob > F	AP
C_f (μg/L)	0.912	0.794	17.620	58.49	56,602.16	7.70	<0.0001	11.3
R_e (%)	0.872	0.710	3.260	3.44	1,933.24	5.06	<0.0001	9.5
ENC (kWh/m^3)	0.991	0.978	0.310	13.79	17.30	78.94	<0.0001	39.5
ELC (kg/m^3)	0.996	0.991	0.001	6.35	0.0002	201.46	<0.0001	60.9
OC ($/m^3)	0.966	0.921	0.130	24.11	3.15	21.36	<0.0001	22.1

The results from the quadratic regression models are expressed in a pair of complex equations. The tested variables are given code values – x_1 to x_7 – and synergistic and antigonistic effects are represented simply by positive and negative signs. The first of the two equations showed R_e (%) was 37.76 and was independent of any other factors, while the linear- (x_1, x_2, x_5, etc.), interaction- (x_1x_3, x_1x_4, x_1x_6, etc.), and second-order terms (x_2, x_3, x_4, etc. [except x_1]) affected the response negatively. Thus As(V) removal efficiency decreased as these terms increased. However, the terms x_6, x_7, x_4, x_3, x_1x_2, x_2x_3, x_1x_5, x_2x_5, x_2x_7, x_3x_5, x_5x_6, x_1^2 had positive influences, denoting an increase in As(V) removal efficiency.

The second equation showed *OC* ($/m^3) and its independent constant was −0.218. The linear- x_2, x_4, x_6, x_7, interaction- x_1x_2, x_1x_5, x_1x_6, x_6x_4, x_2x_5, x_3x_4, x_3x_5, x_3x_6, x_4x_7, x_5x_6, x_6x_7 and second-order terms x_5, x_7 had a negative relationship with the response. However, the linear- x_1, x_3, x_5, interaction- x_1x_3, x_1x_4, x_1x_7, x_3x_2, x_2x_6, x_2x_7, x_3x_7, x_4x_5, x_4x_6, x_5x_7 and second-order terms x_1, x_2, x_3, x_4, x_6 affected the response negatively. As represented in the mathmetical equations, there were significant interaction effects between responses and independent variables. For instance, arsenate removal efficiencies

Downloaded from http://iwaponline.com/wpt/article-pdf/13/4/753/527586/wpt0130753.pdf
by guest

Water Practice & Technology Vol 13 No 4
doi: 10.2166/wpt.2018.088

increased with increases in current density, operating time, and air-flow rate. As the initial As concentration increased, however, removal efficiency decreased.

The current density and operating time were the most important parameters affecting arsenate removal, as Faraday's law controls the dissolution rate of the anodes. Current density is very significant for arsenic removal in EC as it determines the rate of coagulant dosage, size and growth of flocs, and bubble production (Lokendra & Prasenjit 2017). Equation (13) shows that the greater the coagulant concentration, the more current passes through the reactor. Thus, increasing the current density could enhance the concentrations of dissolved Al^{3+} and OH^{-} ions, improving arsenate removal efficiency. This was tested by running a number of experiments at varying current densities (0.1 to 0.5A) – see Table 1 and Figure 2(a) and 2(c)–2(f). The values at 0.1 A for OC, arsenic removal efficiency, and Al/As molar ratio were 0.07 \$/m^3, 95.0% and 155 mol-Al/mol-As, respectively. OC, arsenic removal efficiency, and Al/As molar ratio at 0.5 A were 1.1 \$/m^3, 98.0% and 777 mol-Al/mol-As. OC, arsenic removal efficiency, and Al/As mol ratio increased with increasing current density.

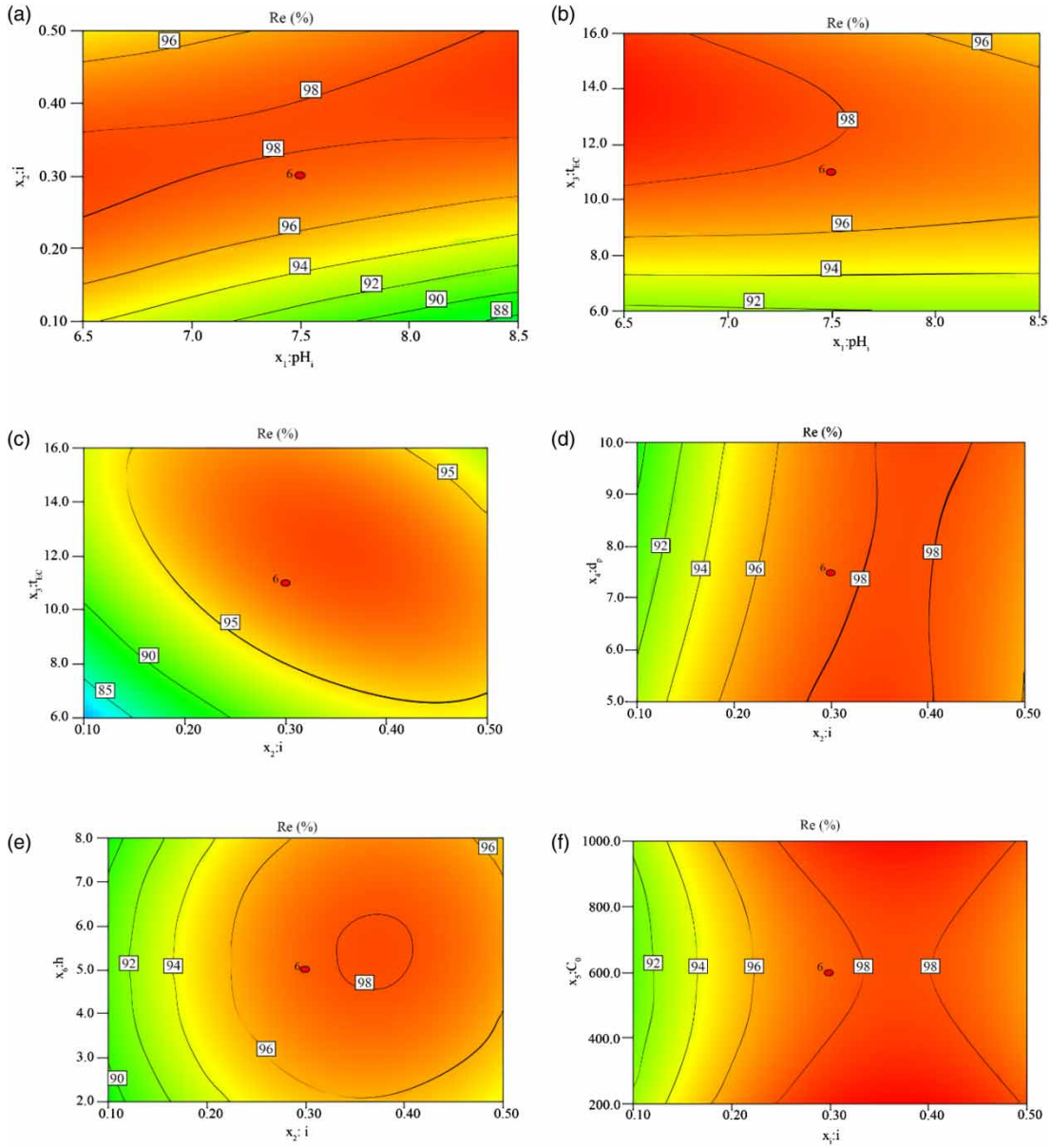

Figure 2 | Two-dimensional contour plots for As(V) removal efficiency vs (a) pH_i-i, (b) t_{EC} – pH_i, (c) *i*-t_{EC}, (d) *i*-d_p, (e) *i*-*h*, and (f) *i*-C_o variables.

Downloaded from http://iwaponline.com/wpt/article-pdf/13/4/753/527586/wpt0130753.pdf
by guest

Water Practice & Technology Vol 13 No 4
doi: 10.2166/wpt.2018.088

Figure 2(a) shows the removal efficiency of arsenic at different current densities (0.1 to 0.5 A). Clearly there was no critical change in removal efficiencies at 0.3 or 0.5 A. However, operating costs and sludge formation also increased with increasing current density. Therefore, taking these into account, EC might best be performed at 0.3 A. The amount of sludge, and the electrode and energy consumptions at 0.1 and 0.5 A, respectively, were 0.05 kg/m^3, −0.0009 kg/m^3, and −0.5 kWh/m^3, and 0.3 kg/m^3, −0.1 kg/m^3, and −9 kWh/m^3. Operating costs at 0.1 and 0.5 A were calculated as 0.1 and 2.2 $/m^3, at 18 minutes, pH_i 7.0, initial arsenic concentration 550 μg/L, column height 8.0 cm, ball size 7.5 mm and air flow rate 6 L/min. Comparisons showed that this study achieved better results than were reported from others. (Parga *et al.* 2005) studied removal of arsenic from groundwater by EC using Al plate electrodes. Their predicted arsenic removal efficiency was 85% at 62.8 minutes operating time, and energy consumption at optimized conditions (pH: 5, A/V: 0.284 cm^2/cm^3, j: 5.78 mA/cm^2, Q_w: 4.3 L/h) was 1.7 kWh/m^3. In a separate study (Alcacio *et al.* 2014), conducted using Al plate electrodes, arsenic removal efficiecny rate was 92.6%. Energy consumption under optimum operating conditions (j: 6 mA/cm^2, As: 134 μg/L, $Q_w = 0$–1 L/min, u = 0.91 cm/s) was calculated as 1.19 kWh/m^3.

Operating time was another parameter affecting arsenic removal in EC. Removal efficiency increased from 93.0% at 2 mins to 99.5% at 18 mins. Similar results were observed in other runs – e.g., 80.2% at 2 mins and 99.0% at 18 mins. Energy and electrode consumptions varied with operating time. At 2 mins they were 0.35 kWh/m^3 and 0.002 kg/m^3, and at 18 mins 3.5 kWh/m^3 and 0.04 kg/m^3. Operating costs were calculated at 0.08 and 0.9 $/m^3, respectively. As described in Equation (14), increased operating times increased the process operating costs.

As can be seen in Figures 2(b) and 2(c), the arsenic removal efficiency at different current densities and pH_i increased with increasing operating time (0 to 16 min). 85% of arsenic was removed in the first six minutes of operation and this rose further to almost 95% at 16 minutes for 0.1 A. 92% arsenic removal efficiency was achieved at pH_i 7.5 in the first six minutes of operation and this increased to 98% at 10 minutes, after which no further change was observed. This indicates that removal efficiency enhancement with increasing operating time arose because of increasing aluminum dissolution. Arsenate ions were available in larger quantities at the beginning of the experiments and formed complexes with aluminum hydroxide easily, leading to rapid arsenate removal early on.

pH is one of the most significant variables affecting arsenate removal. Maximum removal efficiency was just over 99% at pH 5.5 but was below 97% at pH 8.5. Under neutral conditions, Al^{3+} and OH^- react to form various polymeric and monomeric aluminum hydroxide species, which have abundant surface adsorbent areas for arsenic (Kobya *et al.* 2006; Mechelhoff *et al.* 2013). In these conditions, arsenic removal is dominated by precipitation and adsorption, while under basic pH conditions precipitation alone was dominant. The pH values after the experiments were almost 7.5. The insignificant increase in pH associated with the formation of OH^- ions and hydrogen gas at the cathode, stabilised the acid buffer and formed an alkaline solution (Kobya *et al.* 2011).

The interaction of pH and applied current was investigated using the mathematical model. No significant change was observed in the removal of arsenic above pH 7.5 with increase in the applied current (Figure 2(a)). Arsenic removal efficiency also increased with increasing Q_{air} at lower pH values, but decreased with increases in both pH and Q_{air}. For instance, removal efficiency at constant pH 5.5 increased from 87% at 2 L-air/min to 98% at 10 L/min, while removal efficiency at pH 7.0 decreased from 97% at 2 L/min to 86% at 10. Increased air flow rates also reduced electrode consumption and operating costs, while enhancing removal efficiency. Electrode consumption and operating costs were 0.05 kg/m^3 and 1.3 $/m^3 at 2 L-air/min, and 0.03 kg/m^3 and 1.1 $/m^3 at 10 L/min.

The other parameter that affected arsenate removal was the initial arsenic concentration. The effect of this on removal was studied the concentration range 100 to 1,000 μg-As/L. Removal

Downloaded from http://iwaponline.com/wpt/article-pdf/13/4/753/527586/wpt0130753.pdf
by guest

Water Practice & Technology Vol 13 No 4
doi: 10.2166/wpt.2018.088

efficiency fell from 94% at 100 μg/L to 86% at 1,000. The contour plot in Figure 2(d) shows that removal efficiency decreases with increasing initial concentration but increases as the applied current is increased.

Removal efficiency also decreased with increasing aluminum anode ball diameter (Figure 2(d)), varying from 92% at 10 mm to 98% at 5 mm. The 10-minute removal efficiencies for similar operating conditions (pH_i 7.0, ball size 10 mm, current density 0.3 A, initial arsenate concentration 1,000 μg/L and air flow rate 6 L/min) were just under 90% with a column height of 2 cm and just over 92% with a column height of 8 cm. The results from other runs suggest that the total anode surface area decreased with increasing ball size at constant column height, and increased with reactor height at constant ball size. The maximum removal efficiency observed was with an air flow of 6 L/min and 7.5 mm anode ball size. The initial arsenate concentration also affected removal efficiency – e.g., it fell from 99% at 100 μg-As/L to 93% at 1,000 μg/L.

Lower pH values lead to faster and better As(V) removal efficiency. The dissolved aluminum concentration depends on the pH. Thus, at pH 5 to 6, the solubility of aluminum is low and the dominant soluble species are $Al(OH)_4^-$ and Al^{3+}. The As(V) removal efficiency decreases due to the formation of neutrally charged arsenate species and aluminum speciation at high pHs. The As(V) adsorption capacity in the EC process was 5.3 μg-As/mg-Al.

Operating condition optimization

One of the main goals of this work was to determine the optimum values of variables – i.e., to validate the optimum conditions to maximize As(V) removal and minimize operating costs. Design Expert software was operated by setting removal efficiency and operating costs as the goals. In this case, the optimum values of the variables were; pH_i: 6.03, i: 0.11, t_{EC}: 12.5 min, d_p: 10 mm, C_o: 397.4 μg-As/L, h: 5.96 cm and Q_{air}: 5.08 L/min. Under these conditions, the responses were 1.26 μg-As/L effluent arsenic concentration, 99.99% arsenic removal efficiency, 0.25 kWh/m^3 energy consumption, 0.01 kg/m^3 sludge formation, 0.04 \$/m^3 OC and 46.6 μg-As/mg-Al for As (V) adsorption capacity. The final arsenate discharge concentration met the WHO recommendation.

CONCLUSIONS

In this study, BBD was used to optimize As(V) removal from groundwater in a fixed-bed EC reactor using Al-ball anodes. Some 62 experiments were run to develop a quadratic model. The latter provided valid assessments, showing a high regression coefficient between the independent variables and the responses. Of the factors selected, current, operating time, and column height in the EC reactor all have positive effects on As(V) removal. Equally, removal efficiency at low pH values was better than at higher levels, probably because of the increase in Al-floc formation arising from Al speciation at different pHs. At the optimized conditions, the new reactor yielded operating costs of 0.758 \$/m^3 and an arsenate removal efficiency of 99.8%, for an initial concentration of 100 μg-As/L. Thus, the results indicate that the reactor is effective in the removal of both low and high concentrations of As(V) from groundwater.

ACKNOWLEDGEMENTS

The authors would like to thank TÜBİTAK-CAYDAG for their financial support of this work (Contract no: 111Y103).

Downloaded from http://iwaponline.com/wpt/article-pdf/13/4/753/527586/wpt0130753.pdf
by guest

Water Practice & Technology Vol 13 No 4
doi: 10.2166/wpt.2018.088

REFERENCES

Alcacio, R., Nava, J. L., Garreno, G., Elorza, E. & Martinez, F. 2014 Removal of arsenic from a deep well by electrocoagulation in a continuous filter press reactor. *Water Science and Technology: Water Supply* **14**(2), 189–195.

Amrose, S. E., Gadgil, A. J., Srinivasan, V., Kowolik, K., Muller, M., Huang, J. & Kostecki, R. 2009 Arsenic removal from groundwater using iron electrocoagulation: effect of charge dosage rate. *Journal of Environmental Science Health A* **48**(9), 1019.

APHA 2005 *Standard Methods for the Examination of Water and Wastewater*, 21st edn. American Public Health Association/ American Water Works Association/Water Environment Federation, Washington, DC, USA.

Bilici-Baskan, M. & Pala, A. 2010 A statistical experiment design approach for arsenic removal by coagulation process using aluminum sulfate. *Desalination* **254**(1–3), 42–48.

Blangenois, N., Florea, M. & Grange, P. 2004 Influence of the coprecipitation pH on the physicochemical and catalytic properties of vanadium aluminum oxide catalyst. *Applied Catalysis A* **263**(2), 163–170.

Chen, X., Chen, G. & Yue, P. L. 2000 Separation of pollutants from restaurant wastewater by electrocoagulation. *Separation and Purification Technology* **19**(1–2), 65–76.

Çöl, M., Çöl, C., Soran, A., Sayli, B. S. & Öztürk, S. 1999 Arsenic-related Bowen's disease, palmar keratosis, and skin cancer. *Environmental Health Perspectives* **107**(8), 687–689.

Colak, M., Gemici, U. & Tarcan, G. 2003 The effects of colemanite deposits on the arsenic concentrations of soil and groundwater in Igdeköy-Emet, Kütahya, Turkey. *Water Air and Soil Pollution* **149**(1–4), 127–143.

Daneshvar, N., Oladegaragoze, A. & Djafarzadeh, N. 2006 Decolorization of basic dye solutions by electrocoagulation: an investigation of the effect of operational parameters. *Journal of Hazardous Materials* **129**(1–3), 116–122.

Garcia-Lara, A. M. & Montero-Ocampo, C. 2010 Improvement of arsenic electro-removal from underground water by lowering the interference of other ions. *Water Air and Soil Pollution* **205**(1–4), 237–244.

Gomes, J. A. G., Daida, P., Kesmez, M., Weir, M., Moreno, H., Parga, J. R., Irwin, G., McWhinney, H., Grady, T., Peterson, E. & Cocke, D. L. 2007 Arsenic removal by electrocoagulation using combined Al-Fe electrode system and characterization of products. *Journal of Hazardous Materials* **139**(2), 220–231.

Gunduz, O., Simsek, C. & Hasozbek, A. 2010 Arsenic pollution in the groundwater of Simav Plain, Turkey: its impact on water quality and human health. *Water Air Soil Pollution* **205**(1–4), 43–62.

Holt, P. K., Barton, G. W., Wark, M. & Mitchell, C. A. 2002 A quantitative comparison between chemical dosing and electrocoagulation. *Colloids and Surfaces A* **211**(2–3), 233–248.

Kobya, M., Demirbaş, E., Cana, O. T. & Bayramoğlu, M. 2006 Treatment of levafix orange textile dye solution by electrocoagulation. *Journal of Hazardous Materials* **132**(2–3), 183–188.

Kobya, M., Ozyonar, F., Demirbas, E., Sık, E. & Oncel, M. S. 2015 Arsenic removal from groundwater of Sivas- Şarkişla Plain, Turkey by electrocoagulation process: comparing with iron plate and ball electrodes. *Journal of Environmental Chemical Engineering* **3**(2), 1096–1106.

Kobya, M., Ulu, F., Oncel, S. & Demirbas, E. 2011 Removal of arsenic from drinking water by the electrocoagulation using Fe and Al electrodes. *Electrochimica Acta* **56**(14), 5060–5070.

Kumar, P. R., Chaudhari, S., Khilar, K. C. & Mahajan, S. P. 2004 Removal of arsenic from water by electrocoagulation. *Chemosphere* **55**(9), 1245–1252.

Lakshmanan, D., Clifford, D. A. & Samanta, G. 2010 Comparative study of arsenic removal by iron using electrocoagulation and chemical coagulation. *Water Research* **44**(19), 5641–5652.

Lokendra, S. T. & Prasenjit, M. 2017 Simultaneous arsenic and fluoride removal from synthetic and real groundwater by electrocoagulation process: parametric and cost evaluation. *Journal of Environmental Management* **190**, 102–112.

Mechelhoff, M., Kelsall, G. H. & Graham, N. J. D. 2013 Electrochemical behavior of aluminum in electrocoagulation process. *Chemical Engineering Science* **95**, 301–312.

Murcott, S. 2009 *Arsenic Contamination in the World*. IWA Publishing, London, UK.

Ng, J. C., Wang, J. & Shraim, A. 2003 A global health problem caused by arsenic from natural sources. *Chemosphere* **52**(9), 1353–1359.

Nordstrom, D. K. 2015 Worldwide occurrences of arsenic in groundwater. *Science* **296**(5576), 2143–2145.

Parga, J. R., Cocke, D. L., Valenzuela, J. L., Gomes, J. A., Kesmez, M., Irwin, G., Moreno, H. & Weir, M. 2005 Arsenic removal via electrocoagulation from heavy metal contaminated groundwater in La Comarca Lagunera Mexico. *Journal of Hazard Matter* **124**(1–3), 247–254.

Ravenscroft, P., Brammer, H. & Richards, K. 2009 *Arsenic Pollution: A Global Synthesis*. RGS-IBG Book Series, John Wiley and Sons Ltd, London, UK.

Sık, E., Kobya, M., Demirbas, E., Gengec, E. & Oncel, M. S. 2017a Combined effects of co-existing anions on the removal of arsenic from groundwater by electrocoagulation process: optimization through response surface methodology. *Journal of Environmental Chemical Engineering* **5**(4), 3792–3802.

Sık, E., Demirbas, E., Goren, A. Y., Oncel, M. S. & Kobya, M. 2017b Arsenite and arsenate removals from groundwater by electrocoagulation using iron ball anodes: influence of operating parameters. *Journal of Water Process Engineering* **18**, 83–91.

Sık, E., Kobya, M., Demirbas, E., Oncel, M. S. & Goren, A. Y. 2015 Removal of As(V) from groundwater by a new electrocoagulation reactor using Fe ball anodes: optimization of operating parameters. *Desalination and Water Treatment* **56**(5), 1177–1190.

Downloaded from http://iwaponline.com/wpt/article-pdf/13/4/753/527586/wpt0130753.pdf
by guest

Water Practice & Technology Vol 13 No 4
doi: 10.2166/wpt.2018.088

Smedley, P. L. & Kinniburgh, D. G. 2002 A review of the source, behaviour and distribution of arsenic in natural waters. *Applied Geochemistry* **17**(5), 517–568.

Smith, A. H., Lingas, E. O. & Rahman, M. 2000 Contamination of drinking-water by arsenic in Bangladesh: a public health emergency. *Bulletin of the World Health Organization* **78**(9), 1093–1103.

Swamy, G. J., Sangamithra, A. & Chandrasekar, V. 2014 Response surface modeling and process optimization of aqueous extraction of natural pigments from Beta vulgaris using Box-Behnken design of experiments. *Dyes Pigments* **111**, 64–74.

Tseng, C. H., Chong, C. K., Tseng, C. P. & Centeno, J. A. 2007 Blackfoot disease in Taiwan: its link with inorganic arsenic exposure from drinking water. *Ambio* **36**(1), 82–84.

Ucar, C., Bilici-Baskan, M. & Pala, A. 2013 Arsenic removal from drinking water by electrocoagulation using iron electrodes. *Korean Journal of Chemical Engineering* **30**(10), 1889–1895.

Ulu-Kac, F., Kobya, M. & Gengec, E. 2017 Removal of humic acid by fixed-bed electrocoagulation reactor: studies on modelling, adsorption kinetics and HPSEC analyses. *Journal of Electroanalytical Chemistry* **804**, 199–211.

USEPA (United States Environmental Protection Agency) 2001 Drinking Water Standard for Arsenic. EPA-815-F-00-015, Government Printing Office, Washington.

Vaclavikova, M., Gallios, G. P., Hredzak, S. & Jakabsky, S. 2008 Removal of arsenic from water streams: an overview of available techniques. *Clean Technologies Environmental Policy* **10**(1), 89–95.

Vasudevan, S., Lakshmi, J. & Sozhan, G. 2010 Studies on the removal of arsenate by electrochemical coagulation using aluminum alloy anode. *Clean* **38**(5–6), 506–515.

WHO (World Health Organization) 2011 Arsenic in Drinking-water. (Fact Sheet No. 210), Switzerland-Geneva.

Downloaded from http://iwaponline.com/wpt/article-pdf/13/4/753/527586/wpt0130753.pdf
by guest